

Rheological and Calorimetric Evidences of the Fractionated Crystallization of iPP Dispersed in Ethylene/ α -Olefin Copolymers

A. C. MANAURE,^{1*} R. A. MORALES,² J. J. SÁNCHEZ,^{1*} A. J. MÜLLER¹

¹ Grupo de Polímeros U.S.B., Departamento de Ciencia de los Materiales

² Departamento de Mecánica, Universidad Simón Bolívar, Apartado 89000, Caracas 1080-A, Venezuela

Received 5 February 1997; accepted 26 June 1997

ABSTRACT: In this work, the melt crystallization of immiscible blends of isotactic polypropylene (iPP) and branched polyethylenes (PE) was followed by oscillatory shear measurements during controlled cooling. All the blends contained 20% iPP finely dispersed in several ethylene/ α -olefin copolymer matrices (with and without a nucleating agent) with densities ranging from 0.88 to 0.92 g/cm³ (linear low, very low, and ultra low density polyethylenes: LLDPE, VLDPE, and ULDPE). The rheological results were compared with parallel differential scanning calorimetry (DSC) measurements at the same cooling rate. During preliminary evaluations of the neat resins, no effect was found of the variation of the frequency of oscillation or the applied shear strain on their crystallization (at least in the range explored in this work). In the case of the blends, when the iPP crystallized in a fractionated fashion, only one sudden increase in the storage modulus (G') was observed during cooling due to the partial coincident crystallization of both iPP and the PE matrix. In the presence of a nucleating agent, an almost complete separation between the crystallization of both components in the blend was achieved and two increases in G' were clearly observed upon cooling. A close match between the dynamic crystallization kinetics obtained by DSC and torsion rheometry was demonstrated by a direct comparison between calorimetrically measured solid conversion and G' during cooling from the melt. © 1997 John Wiley & Sons, Inc. *J Appl Polym Sci* **66**: 2481–2493, 1997

Key words: fractionated crystallization; branched PE/PP blends; dynamic rheological measurements; ultra low density polyethylene; very low density polyethylene

INTRODUCTION

In recent years the rheological properties of immiscible polymer blends, at temperatures where one of the components can crystallize while the other is molten, have been reported. These rheological evaluations have been performed on isotac-

tic polypropylene (iPP) and high density polyethylene (HDPE) blends at isothermal and dynamic crystallization conditions of the dispersed minority phase.^{1,2} Similar studies have also been published^{2–6} for pure polymers (e.g., HDPE, iPP, and Nylon 6) or mixtures of polymers and nucleating agents, where the rheological measurements are carried out at temperatures at which only part of the crystallinity has developed and most of the polymer is still in the melt state. On the other hand, Hingmann, Rieger, and Kersting⁷ have used rheological measurements to investigate the phenomenon of lamellar thickening in random copolymers of iPP where annealing has been per-

Correspondence to: A. J. Müller.

* Present Address: Investigación y Desarrollo C.A., INDE-SCA, Complejo Petroquímico Zulia, El Tablazo, Edo. Zulia, Venezuela.

Journal of Applied Polymer Science, Vol. 66, 2481–2493 (1997)
© 1997 John Wiley & Sons, Inc. CCC 0021-8995/97/132481-13

formed at a temperature where partial melting has occurred.

In all the studies quoted above, the rheological behavior of the system under investigation was found to be similar to that of a filled polymer, where the polymer crystallites act as the filler. In a typical filled polymer, the real nature of the polymer–filler interface is generally unknown and the filler particles are usually anisotropic. This can make the modeling of these systems quite complex, a fact that can prompt the use of spherical filler particles and interfacial agents. The advantage of a partially crystallized polymer where its own crystals act as fillers is the fact that the filler can be considered as spherical entities (i.e., spherulites) that exhibit a perfect adhesion with the matrix, since the melted amorphous phase is connected with the supercrystalline structure.⁵

In view of the fact that part of the polymer (or one component in a blend) is crystallizing during the course of the rheological measurement, the data gathered contains information on the crystallization kinetics. Therefore, some authors have made efforts to correlate these data with other crystallization kinetic parameters obtained by differential scanning calorimetry (DSC) and polarized light microscopy (PLM).^{2,6}

The crystallization process in polymers is usually followed by techniques that measure changes that are directly related to the progress of crystallinity, such as enthalpic changes (DSC), volumetric differences (dilatometry), spherulitic growth (PLM), and lamellar and/or superstructure development (small angle light scattering, X-ray diffraction, Raman spectroscopy, and small angle neutron scattering).^{8–11} In all these cases the experimental variables associated with these techniques (apart from the expected kinetic dependencies with cooling rates) do not affect the crystallization process. When the crystallization is followed by dynamic rheological techniques, like oscillatory shear, the sample is exposed to a fixed deformation (γ) at a particular frequency (ω). It is then possible that the action of this simple shear flow field affects the crystallization process depending on the magnitude of γ and ω . Furthermore, it is well known that the rheological properties in oscillatory shear must be measured under experimental conditions where the material is within the linear viscoelastic range, in order to ensure that the measured properties are only a function of frequency and temperature and not of deformation.¹² These conditions are easy to establish in the melt in homogeneous materials

but not in heterogeneous media, especially if the structure of the melt changes during the measurement, as in the case of a crystallizing polymer.⁵ Nevertheless, under equivalent experimental conditions, the registered rheological properties could yield complementary information of the crystallization kinetics of complex systems.

Teh, Blom, and Rudin² and Carrot, Guillet, and Boutahar⁵ have pointed out that during rheological measurements on crystallizing systems, the applied strain must be low enough to avoid any possible perturbation of the crystallization kinetics. Teh, Blom, and Rudin also indicate that the same precaution should be applied to the frequency, while from an instrumental point of view the measurements should be made in a long enough time interval during crystallization before the torque or load limit of the transducer is reached. They performed dynamic and isothermal rheological measurements on iPP, HDPE, and iPP/HDPE blends (in the composition range where iPP was the matrix) using the following constant experimental conditions: $\omega = 1 \text{ rad s}^{-1}$ and $\gamma = 0.8\%$. On the other hand, Carrot, Guillet, and Boutahar also used a constant frequency of 1 rad/s but reported that changes in strain from 0.02% to 25% did not affect the crystallization process. Shroff, Prasad, and Lee⁶ only adjusted their frequency (between 10 and 50 rad s^{-1}) and strain values (between 3 and 5%) to optimize their signal-to-noise ratios on their rheological measurements of different HDPE grades.

The phenomenon of fractionated crystallization has been the subject of several recent investigations.^{13–26} Commercial polymers are generally nucleated by heterogeneities that are usually present in them and can effectively induce crystallization at a specific undercooling. When a crystallizable polymer is very finely dispersed in an immiscible matrix, such that the number of dispersed particles is much greater than the number of heterogeneities that usually nucleate the polymer in bulk at a specific undercooling, the polymer crystallization usually occurs in one or more stages at substantially larger undercoolings than those needed to crystallize the same polymer in bulk. The reason behind such fractionated crystallization is that only a small fraction of polymer droplets will contain the highly active heterogeneities capable of nucleating the polymer at high temperatures, and therefore the rest of the droplets will need higher undercoolings in order to activate other types of less efficient heterogeneities and/or eventually produce homogeneous nucleation. A thorough review of earlier literature on

the subject was published by Frensch, Harnischfeger, and Jungnickel in 1988.¹³ In recent years we have made some effort to understand the fractionated crystallization process of polyolefins dispersed in several immiscible matrices. The phenomenon has been mainly studied in our group by DSC using several approaches, such as self-nucleation^{18,19,26} or the addition of nucleating agents.^{16,17,20,26} The influence of mixing variables,¹⁸ blend type,^{24–26} and the possible effects on the mechanical and dynamic mechanical properties^{18–20,23} of the blends has also been investigated.

In the present work, we continue our studies on the fractionated crystallization of iPP dispersed in several immiscible matrices of branched polyethylenes by the use of torsional rheometry to determine dynamic rheological properties upon controlled cooling from the melt. For comparison purposes we have also used analogous blends with a nucleating agent where the fractionated crystallization is not present. Before determining the conditions of frequency and strain to be used in the rheological measurements with the blends, a preliminary evaluation of the effect of these variables on the neat resins was made. The results were compared with parallel dynamic DSC determinations at identical cooling rates.

EXPERIMENTAL

Materials

The materials used in this study were a linear low density polyethylene (LLDPE) ethylene/1-butene copolymer SCLAIR 11U4, manufactured by DuPont Canada, a very and an ultra low density polyethylene (VLDPE and ULDPE), NVLD1 and NULD1, ethylene/propene/1-butene copolymers of Enichem Polimeri (Italy), an isotactic polypropylene (iPP) J400 manufactured by Polipropilenos de Venezuela (Propilven), and sorbitol as a nucleating agent. Table I lists some characteristic properties of these materials.

Blend Preparation

The polymers were melt-mixed in a Haake Rheocord EU10 co-rotating twin screw extruder at 210°C and 40 rpm. The blending temperature and deformation rate were selected from an extrapolation of capillary rheometry experiments on the neat resins by choosing a viscosity ratio of the polymers to be mixed as close to one as possible.

The branched PE/iPP blends were prepared at a constant composition weight/weight ratio of 80 : 20. Blends of similar composition with 0.1% by total weight of sorbitol were also prepared.

Dynamic Rheological Measurements

The dynamic rheological measurements were performed in a Rheometrics RDA II under dynamic temperature ramp mode operation, using plate-plate geometry (25 mm diameter) and a gap of 1.8 mm. The samples were circles cut from sheets previously molded by compression at 170°C with a nominal thickness of 2.0 mm. The effect of specimen dimensions in torsion rheometry (using a plate-plate geometry) has been examined in the literature.^{5,6} When the polymer crystallizes, a substantial volume contraction can occur depending on how much the sample crystallizes before the test is stopped. In case the contraction is substantial, two effects can be present.⁵ On one hand the sample could be submitted to a tensile force between the plates if the distance between the plates is kept constant (as is usually the case), and on the other hand, the diameter of the sample between the plates could be lower than its initial value. These dimensional changes could induce errors in the quantitative estimations of rheological properties that are calculated from torque measurements (such as storage modulus, G'). Carrot, Guillet, and Boutahar⁵ proposed that the distance between the measuring plates should be adjusted while the crystallization process is proceeding such that a negligible value of normal forces is registered during the run (such adjustment must then be taken into account in the calculations of the rheological properties). Since the primary objective of the present work is to study the crystallization of 20% of the sample, which is well dispersed in a molten matrix, we did not correct our measurements for sample contraction. The only results presented here which may contain an appreciable error in this respect are those of the neat resins; however, internal comparisons between the runs should still be valid even if the exact quantitative values may contain slight errors.

In this work we have prepared samples of a starting nominal thickness of 2 mm, a value commonly used for rheological determinations in order to obtain a good signal-to-noise ratio. Since the temperature control in the RDA is not the same as in an adiabatic calorimeter like a DSC, there will be differences in temperature distribution throughout the sample in both methods. These will be considered in the discussion below.

Table I Selected Properties of the Resins Used in This Study

Material	Density (g/cm ³)	MFI ^(a) (dg/min)	Molecular Weight (g/mol)	Branch Content (mol %)
LLDPE SCLAIR 11U4	0.922	1.4	\bar{M}_n : 37,800 \bar{M}_w : 159,700	Ethyl: 2.5
VLDPE NVLD1	0.903	3.1	—	—
ULDPE NULD1	0.888	2.1	\bar{M}_n : 23,000	Methyl: 8.7 Ethyl: 5.2
iPP J400	0.910	3.0	—	—

^a ASTM D 1238: PE 190°C and iPP 230°C.

In fact, Shroff, Prasad, and Lee,⁶ in a very recent work, recommend the use of very thin samples (0.6 mm or less) in order to ensure a good temperature distribution throughout the sample.

The cooling rate employed was 5°C min⁻¹, all the samples were heated to 200°C for 3 min before starting the cooling run in order to erase all previous thermal history, and the temperature was measured on the lower plate of the measuring device. To evaluate the effect of deformation on dynamic crystallization in pure polymers, several tests were performed in a range from 0.8% to 25% (all of them within the linear viscoelastic regime before the onset of crystallization) at a constant frequency of 1 rad s⁻¹. Also, the effect of frequency was evaluated in a range from 0.5 to 100 rad s⁻¹ at a constant deformation of 1.0%. All tests were repeated three times to check reproducibility.

After evaluating the pure polymers, specific values of frequency and strain were chosen for testing all the blends (5 rad s⁻¹ and 1.0% strain), these were chosen as the conditions where the effect of such variables over the crystallization kinetics of the materials tested in this work was negligible (see Table II below).

Additionally, dynamic frequency sweep tests under isothermal conditions for all blends were performed applying a constant deformation of 15% in the range 10⁻¹–10² rad s⁻¹ at different temperatures: 120, 130, and 150°C, following a period of 3 min in the melt at 200°C.

Differential Scanning Calorimetry

A Perkin–Elmer DSC7 was used for calorimetric evaluations. The cooling rate of the DSC experiments was identical to that used in the rheometer (i.e., 5°C min⁻¹). High purity dry nitrogen was used as an inert atmosphere and the sample weight was 10 mg for all the samples examined.

An “unmixed blend” (u.b.) sample was used in order to have a reference cooling scan. Such a sample was prepared using the same weight proportion of pure polymers in the blends without nucleating agent, but placing both polymers in a DSC pan separated by aluminum foil [i.e., with no contact whatsoever between the two polymers (see refs. 18 and 27)]. The heat of crystallization (ΔH_c) for 100% crystalline materials was taken as 293 J g⁻¹ and 207 J g⁻¹ for PE and iPP, respectively.²⁸

RESULTS AND DISCUSSION

Effect of the Strain and Frequency on the Dynamic Crystallization of Pure Polymers

The crystallization behavior of the neat resins is presented in Figure 1(a), where the DSC cooling runs at the same cooling rate used in the RDA are shown. Figure 1(b) presents the data of Figure 1(a) transformed to crystallinity versus temperature by partial integration and the use of 100% crystallinity ΔH_c values (see Experimental section and ref. 28). The iPP exhibits a very sharp crystallization exotherm characteristic of the material. The content and heterogeneous distribution of chain branching in the ethylene/ α -olefin copolymers produces chain segregation during crystallization,^{8,29} whereby the more linear chains of the distribution crystallize at higher temperatures in a relatively sharp exotherm [Fig. 1(a)], and the less linear chains crystallize at lower temperatures in a broad tail or shoulder. In the case of the VLDPE and the ULDPE, crystallization can continue even below room temperature.³⁰ In Figure 1(b) the region of maximum slope corresponds to the first high temperature exotherm in Figure 1(a) for each polymer. Figure 1(b) shows

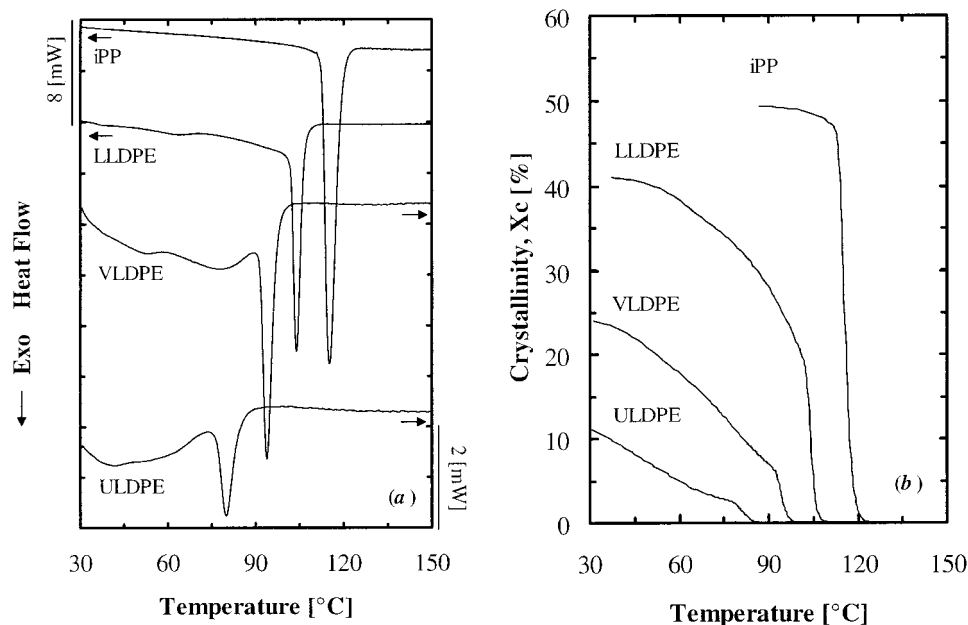


Figure 1 (a) DSC cooling curves of neat polymers cooled at 5°C/min from 200°C, and (b) crystallinity X_c versus temperature, obtained by partial integration of the DSC traces in (a).

how the iPP crystallizes up to nearly 50% in a few degrees, while the LLDPE develops 20% crystallinity also in a very narrow temperature range and then keeps crystallizing at lower temperatures until at 30°C it possesses $\sim 40\%$ crystallinity. In the case of the VLDPE or the ULDPE the high temperature first exotherm only amounts to the development of very modest crystallinity degrees. In the case of ULDPE, the polymer only contains $\sim 11\%$ crystallinity at room temperature, therefore displaying rubbery behavior.

Figure 2 shows examples of G' versus temperature curves for the neat resins along with a superposition of the crystallinity data presented in Figure 1(b). This representation demonstrates that any increase in crystallinity will result in a proportional increase in G' , as should be expected. It can be observed that upon cooling from the melt, the values of G' monotonically increase as the temperature is decreased until a temperature is reached where the polymer starts crystallizing and a dramatic increase in G' occurs over a very narrow temperature range. If one extrapolates the region of maximum slope to the region where the G' curve is changing slowly with temperature, an onset value is obtained in an analogous way to DSC onset temperature determinations (i.e., onset crystallization, vitrification, or melting²⁸). In the case of LLDPE and iPP in Figure 2(a), the run had to be stopped shortly after crystallization

had started since the normal force measurement was overloaded before the completion of the crystallization. It must be taken into account that these two polymers crystallize very fast in a relatively narrow temperature range and up to high degrees of crystallinity (Fig. 1). For these reasons the matching between the crystallinity data obtained by DSC and the G' data obtained by RDA is not perfect, even if there is a very good qualitative agreement. A small temperature difference can cause a significant horizontal displacement between the curves in the region where either iPP or LLDPE are crystallizing. In the case of the LLDPE it is probable that the test was stopped when the crystallinity level was around 20% (as indicated by DSC data) if the change in slope in the RDA data at the lowest temperature range is considered.

Figure 2(b) shows the comparison between DSC and RDA measurements for the VLDPE and the ULDPE. The agreement is very good. In this case, because the crystallinity achieved by these polymers is lower than for iPP or LLDPE, the RDA measurements could encompass much lower temperatures. For the ULDPE, the crystallization of the high temperature exotherm (see Fig. 1) that corresponds to $\sim 3\%$ crystallinity was followed by a proportional increase in G' , and further crystallization was registered down to 60°C.

Table II presents data on the influence of defor-

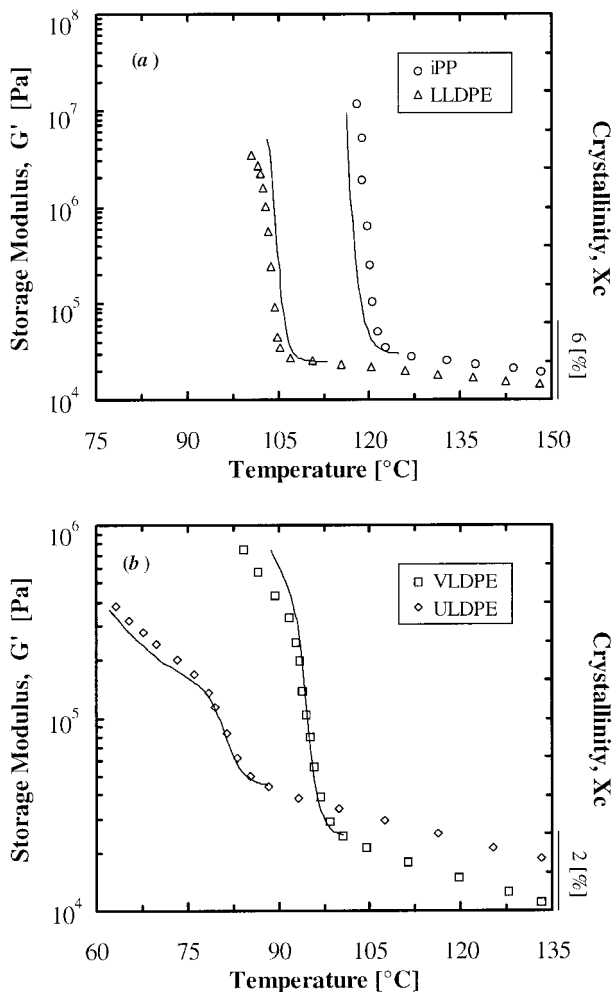


Figure 2 DSC derived crystallinity curves (solid line) and storage modulus G' at 5 rad/s and strain of 1% (symbols) versus temperature during cooling at 5 $^{\circ}\text{C}/\text{min}$: (a) iPP, LLDPE, and (b) VLDPE, ULDPE.

mation (γ) and frequency (ω) over the dynamic crystallization of LLDPE, ULDPE, and iPP at 5 $^{\circ}\text{C}/\text{min}$. Equivalent results were obtained at 2.5 $^{\circ}\text{C}/\text{min}$.²¹ The table presents the onset crystallization temperature obtained from the change observed in the curves of G' as a function of temperature, as described previously and also values obtained by DSC. Figure 3 shows examples of G' versus temperature curves for two frequencies at constant strain. It can be observed in Table II that the onset crystallization temperature is not affected at all by changing the applied strain in the range explored in this work. The effect of frequency of deformation is also not significant except at very low frequencies, where a small increase in the onset temperature ($\sim 2^{\circ}\text{C}$ for LLDPE and 1°C for ULDPE) was detected. For iPP at 0.5 rad s^{-1} the onset crystallization temperature cannot

be determined by RDA [Fig. 3(b)]. When the RDA dynamic cooling run is performed at a frequency of 0.5 rad s^{-1} [Fig. 3(b)] there is a mismatch between the frequency at which the measurements is performed and the crystallization time upon cooling. The time needed for the instrument to complete a full cycle and register an experimental point could be longer than the mean crystallization time at that temperature interval, especially when the crystallization rate increases upon cooling. Because of this only a few data points are actually measured; as a matter of fact, all the available data points were plotted in Figure 3(b) for the measurements made at 0.5 rad s^{-1} , while in all the other RDA curves presented in this work we have included fewer data points than actually measured in the interest of clarity. In the case of LLDPE at 0.5 rad s^{-1} [Fig. 3(b)] only two points define the region where G' increases to very high values, while in the case of iPP the polymer crystallized so fast that the experiment had to be stopped by overload before a data point in the region of high G' was taken. In the case of ULDPE at 0.5 rad s^{-1} [Fig. 3(b)], since the polymer crystallizes at a lower rate and up to a lower extent, the measurement frequency is faster than the rate at which G' is increasing due to crystallization, then the curve was fully registered.

According to the results gathered here, the frequency and strain (in the range explored in this work) are not affecting the crystallization behavior of the materials under investigation if the frequency is kept at high enough values that allow measurements during crystallization. In view of the above results, a frequency of 5 rad s^{-1} and a strain of 1.0% were chosen in order to study the behavior of the blends.

When the onset crystallization temperatures obtained by RDA measurements are compared to those obtained by DSC for the neat resins (Table II), it can be seen that there is in general very good agreement between both measurements. Teh, Blom, and Rudin² have reported similar results on the dynamic crystallization of iPP; however, they claimed that a nucleation stage could be detected by RDA, since a slight increase in G' was observed at high temperatures ($\sim 150^{\circ}\text{C}$) before any exothermic signal could be detected at equivalent temperatures in the DSC. They argued that such nucleation could only be detected by RDA measurements at cooling rates that were lower or equal to 2 $^{\circ}\text{C}/\text{min}$. In our case we were not able to detect this nucleation signal in iPP at 5 $^{\circ}\text{C}/\text{min}$ or at 2.5 $^{\circ}\text{C}/\text{min}$; we did not use

Table II Effect of Frequency and Strain on Onset Crystallization Temperatures Obtained by Rheological and Calorimetric Measurements in LLDPE, ULDPE, and iPP

Parameter	T_c Onset		
	LLDPE	ULDPE	iPP
Frequency (rad s ⁻¹)			
0.5	108.3 ± 0.3	86.3	—
1.0	106.7 ± 0.6	85.3 ± 0.3	122.0 ± 0.5
5.0	105.6 ± 0.2	85.8 ± 0.6	122.0 ± 0.6
10.0	105.3 ± 0.1	85.6 ± 0.7	121.7 ± 0.2
50.0	105.3 ± 0.1	85.7 ± 0.2	121.7 ± 0.1
100.0	105.7 ± 0.2	84.5 ± 0.1	121.6 ± 0.6
Strain (%)			
0.8	106.5	85.0 ± 0.8	124.4 ± 0.2
1.0	106.7 ± 0.6	85.3 ± 0.3	122.0 ± 0.5
5.0	106.7 ± 0.3	85.0 ± 0.8	122.5 ± 0.7
10.0	106.6 ± 0.4	85.6 ± 0.2	122.0 ± 0.8
15.0	106.5 ± 0.2	85.5 ± 0.2	121.0 ± 0.3
20.0	106.5 ± 0.2	85.7 ± 0.4	122.2 ± 0.4
DSC	106.5	85.0	119.3

lower cooling rates. Even with the addition of a nucleating agent we were not able to observe a similar behavior to that reported by Teh, Blom, and Rudin.

Finally, it is worth mentioning that the experimental variable that generally limited the lowest temperature achieved in the RDA measurements on the neat resins was the saturation of the normal force rather than a torque overload. This result is in agreement with those of Carrot, Guillet, and Boutahar,⁵ since they indicated that the volumetric contraction experienced by the crystallizing sample (especially in the case of iPP and LLDPE) had an effect on the normal force experienced by the sample.

Fractionated Crystallization of Polypropylene Dispersed in an Immiscible Polymeric Matrix

When 20% of iPP was melt mixed with any of the ethylene/ α -olefin copolymers used in this work, a very good dispersion of iPP droplets in a branched PE matrix was produced. Scanning electron microscopy (SEM) of cryogenically fractured specimens showed that the mean particle size was of the order of 1 μ m or less. An estimation of the number of particles per unit volume gave values of the order of 10¹² particles/cm³, while the number of heterogeneities measured by PLM in the iPP used here was only in the order of 10⁶ heterogeneities/cm³. These were ideal conditions for the

occurrence of the fractionated crystallization phenomenon that we had described previously.^{16,18}

Figure 4 presents the DSC cooling behavior (at 5°C min⁻¹) of the neat resins and the blends with and without sorbitol, the onset crystallization temperature of each sample is given in Table III along with the peak crystallization temperature of the first exotherm (i.e., that located at the highest temperature). If the blends were immiscible and blending had no effect on the crystallization behavior of the pure components, then the DSC cooling scans should closely resemble those of the 80 : 20 LLDPE/iPP, VLDPE/iPP, and ULDPE/iPP unmixed blends (u.b.) shown in Figure 4(a–c). In all unmixed blends the crystallization exotherm of each component is clearly identified by the different crystallization temperature range of iPP and any of the branched PE's, and the 80 : 20 composition is reflected in the size of each exotherm.

In contrast to the unmixed blend behavior, the real melt-mixed LLDPE/iPP blend without sorbitol [80 : 20 : 0 in Fig. 4(a)], exhibited only one crystallization exotherm at an intermediate temperature between those of the pure polymers. We have demonstrated^{20,26} that this is due to coincident crystallization, a special case of fractionated crystallization.¹³ The iPP crystallized in a fractionated fashion, therefore lowering its crystallization temperature in such a way that it overlapped with the LLDPE exotherm. However, once the iPP droplets started to crystallize they nucle-

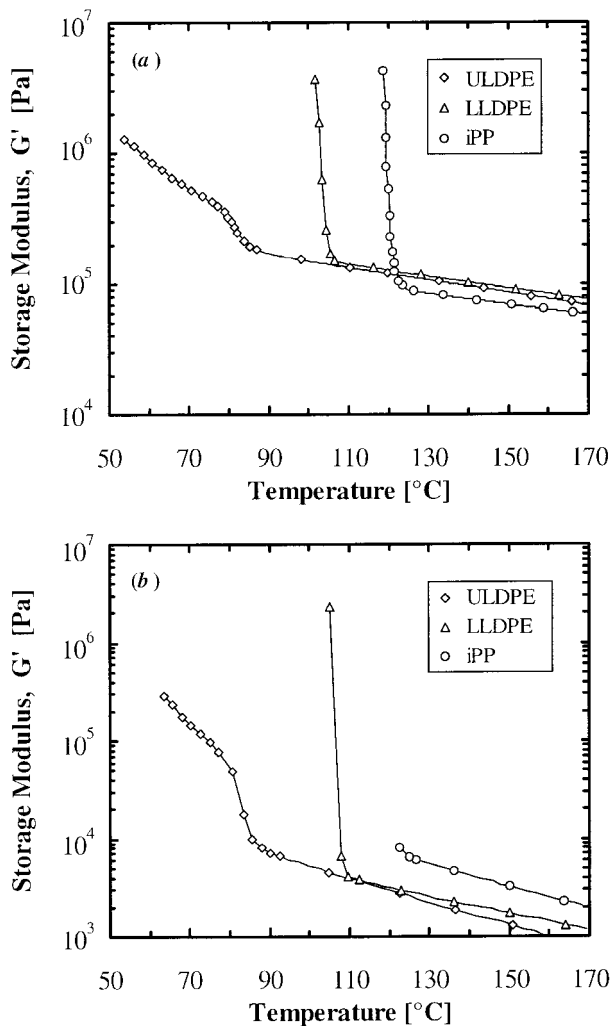


Figure 3 Storage modulus G' versus temperature during cooling at $5^\circ\text{C}/\text{min}$ for ULDPE, LLDPE, and iPP, at a constant applied strain of 1%: (a) 50 rad s^{-1} and (b) 5 rad s^{-1} .

ated the LLDPE matrix, therefore causing the only discernible crystallization peak to be 3.7°C higher than that of the pure LLDPE.

Figure 4(a) also offers evidence that the effect described above is indeed due to fractionated crystallization, that is, to the fact that the number of dispersed iPP droplets in the LLDPE matrix is much greater than the number of heterogeneities originally present in the bulk iPP.¹⁸ When sorbitol was added to the LLDPE/iPP blend [80 : 20 : 0.1 sample in Fig. 4(a)], the fractionated crystallization disappeared, since the sorbitol provided the heterogeneous nuclei that all the iPP droplets needed in order to crystallize at similar temperatures to that of pure iPP with sorbitol. In this sample the exotherms corresponding to the crystallization of the two components in the blend

were clearly separated. Moreover, an additional nucleation effect of LLDPE had been induced by the iPP/sorbitol mixture, causing a substantial increase in the LLDPE crystallization peak temperature [8°C higher than pure LLDPE, compare in Fig. 4(a) the 100 : 0 : 0 and the 80 : 20 : 0.1 curves]. The widening of the LLDPE exotherm upon addition of sorbitol suggests that a preferential nucleation of the more linear chains within the wide distribution of chain branching present in the LLDPE could take place.

The fractionated crystallization of iPP also occurs when the polymer is dispersed in highly branched PE such as VLDPE [Fig. 4(b)] or ULDPE [Fig. 4(c)]. In Figure 4(b) the depression of the crystallization temperature of iPP when it is dispersed in VLDPE is even more noticeable than when it is dispersed in LLDPE. When the unblended sample is compared to the melt-mixed 80 : 20 : 0 VLDPE/iPP blend, the absence of the high temperature exotherm of iPP is very clear. The DSC trace of the real 80 : 20 : 0 melt mixed blend is very complex; it contains several peaks and shoulders. If one looks closer to that trace, it can be noticed that the first exotherm that is encountered upon cooling has a high temperature shoulder which could reflect the first part of the fractionated crystallization of iPP, while the actual peak could correspond to the crystallization of the VLDPE that is being nucleated by the iPP. Then, a series of secondary peaks follow at lower temperatures; these peaks are due to the crystallization of the rest of the VLDPE overlapped with other fractions of iPP that can also be crystallizing at lower temperatures. When the nucleating agent is added to the blend, the iPP component crystallizes at higher temperatures as expected, while the VLDPE matrix is nucleated by the iPP/sorbitol, thereby causing a broadening of its exotherm in comparison to that of the original VLDPE (as a matter of fact, the high temperature exotherm of pure VLDPE located at $\sim 90^\circ\text{C}$ is so spread out in the 80 : 20 mixture with sorbitol that it cannot be detected anymore).

A very similar behavior to that described above for the fractionated crystallization of the iPP in a VLDPE matrix is displayed in Figure 4(c) for the case of an ULDPE matrix. The qualitative behavior was nearly identical, but quantitatively the crystallization temperatures of iPP and ULDPE for the unmixed blend were even more separated. This made the fractionated crystallization very apparent, since the onset crystallization temperature of the melt-mixed blend [80 : 20 : 0 in Fig. 4(c)] was displaced to lower temperatures at least

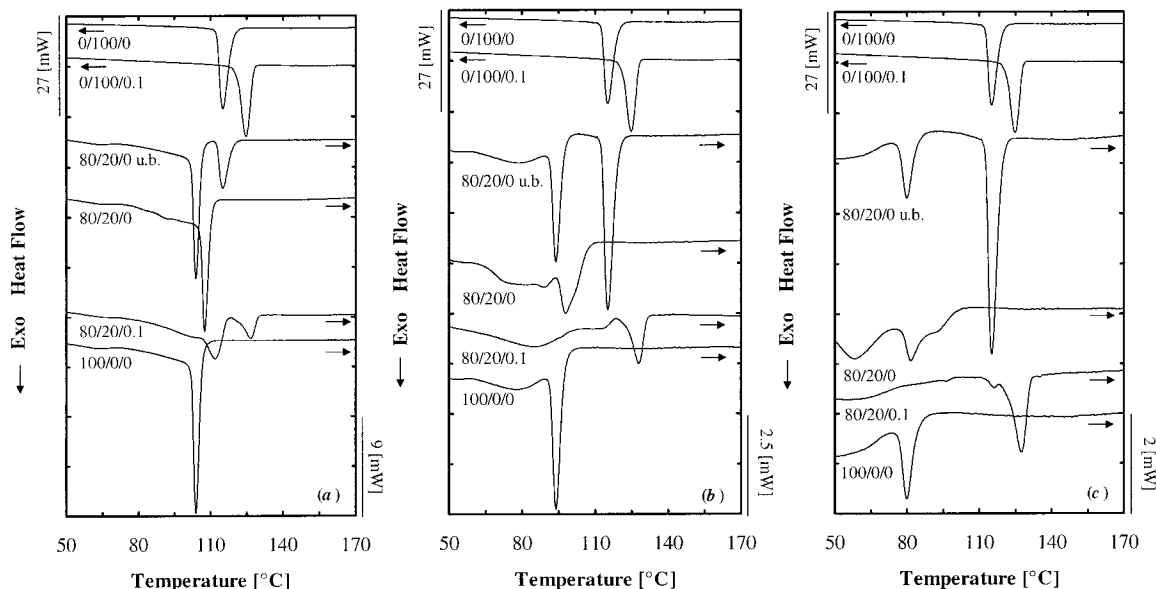


Figure 4 DSC cooling curves at 5°C/min from 200°C for: (a) LLDPE/iPP/sorbitol blends, (b) VLDPE/iPP/sorbitol blends, and (c) ULDPE/iPP/sorbitol blends. u.b.: un-mixed blend.

15°C with respect to the un-mixed blend. In this system once again the fractionated crystallization disappeared upon addition of sorbitol. The crystallization of the ULDPE component in the

80 : 20 : 0.1 blend was extremely broad and started at higher temperatures with respect to that of pure ULDPE in view of its nucleation by sorbitol. Such behavior was also observed in samples of pure ULDPE with sorbitol.²⁶

Table III Crystallization Temperatures Obtained by DSC and RDA

	DSC (°C)		RDA (°C)
	T_p^a	T_0^b	T_0^b
LLDPE/iPP/sorbitol			
100 : 0 : 0	103.9	106.5	105.5
100 : 0 : 0.1	105.3	115.4	—
80 : 20 : 0	107.7	110.4	109.1
80 : 20 : 0.1	126.9	129.3	130.7
0 : 100 : 0	115.2	119.3	121.1
0 : 100 : 0.1	124.5	128.0	129.9
VLDPE/iPP/sorbitol			
100 : 0 : 0	93.9	97.4	97.7
100 : 0 : 0.1	84.2	116.5	—
80 : 20 : 0	97.8	107.8	108.9
80 : 20 : 0.1	127.8	131.0	131.8
ULDPE/iPP/sorbitol			
100 : 0 : 0	80.1	85.0	85.9
100 : 0 : 0.1	49.6	113.1	—
80 : 20 : 0	81.6	101.1	114
80 : 20 : 0.1	127.3	130.9	133

^a T_p : Peak crystallization temperature of the highest temperature exotherm.

^b T_0 : Maximum onset crystallization temperature.

Evidences of Fractionated Crystallization by Rheological Measurements

In this section we present, as far as we are aware, for the first time (with the exception of a couple of preliminary reports by our group^{21,22}) results on the rheological consequences of the fractionated crystallization. Figure 5 shows the variation of storage modulus G' with temperature during cooling at 5°C min⁻¹ for two of the systems under investigation (i.e., LLDPE/iPP and VLDPE/iPP). As mentioned above, the sudden rise in G' upon cooling from the melt indicated the onset of crystallization in the sample. For all the systems evaluated, the onset temperatures were in close agreement with the onset of crystallization as determined by DSC and shown in Table III. As indicated in this table, we were not able to identify significant differences in the onset temperatures by DSC and RDA that could be attributed to differences in technique sensitivity to the nucleation and crystallization processes as suggested by Teh, Blom, and Rudin.²

From Figure 5(a) or (b) it is apparent that the first polymer to crystallize upon cooling, thanks

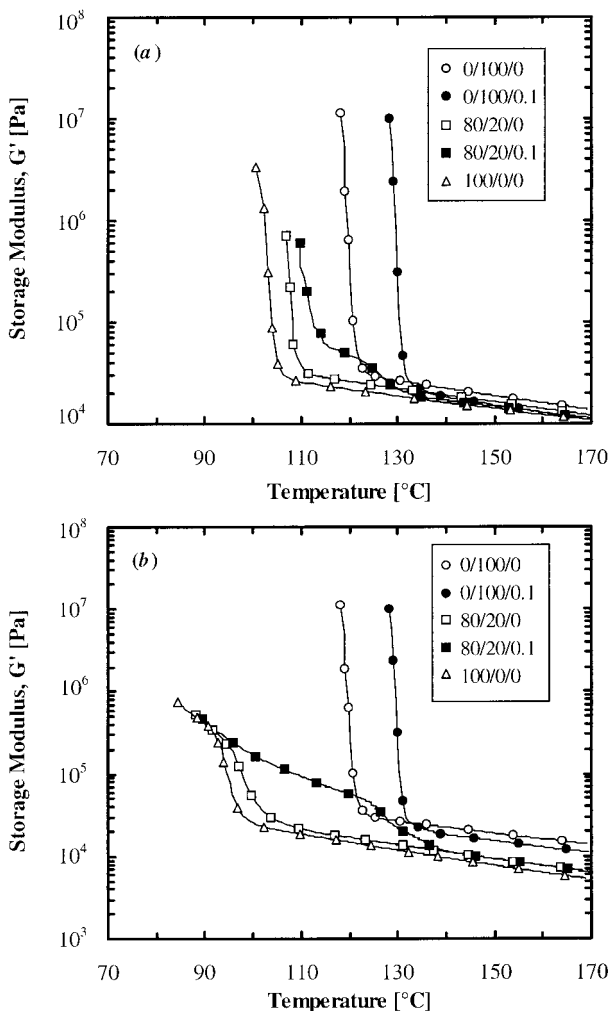


Figure 5 Storage modulus G' versus temperature during cooling at $5^{\circ}\text{C}/\text{min}$ for: (a) LLDPE/iPP/sorbitol blends and (b) VLDPE/iPP/sorbitol blends. Frequency: 5 rad s^{-1} , Strain: 1%.

to the sorbitol, is iPP with sorbitol (at 129.9°C , see Table III). The iPP without nucleating agent crystallizes as expected at lower temperatures (at 121.1°C). In Figure 5(a and b) the curves that correspond to the 80 : 20 LLDPE/iPP and VLDPE/iPP blends with sorbitol are the most peculiar. In both systems, the samples upon cooling [compare with the corresponding DSC curves in Fig. 4(a) and (b)] experience a gradual and modest increase in G' from an onset temperature which is close to that of pure iPP with sorbitol (at $\sim 129.9^{\circ}\text{C}$). The G' suddenly increases with decreasing temperature from 115°C onward for the LLDPE/iPP blend with sorbitol, while the VLDPE/iPP blend with sorbitol only displays a second gradual increment in G' at around the same temperature. We attribute the first gradual

rise to the crystallization of the iPP dispersed droplets (since iPP only amounts to 20% weight fraction and it conforms the dispersed phase, a comparatively smaller increase in G' is expected) within the molten LLDPE and VLDPE matrix. In the case of LLDPE/iPP/sorbitol blend, the second very sudden rise in G' upon cooling corresponds to the onset of crystallization of the LLDPE matrix. For the VLDPE/iPP/sorbitol blend, the second rise in G' upon cooling is more gradual since it is due to the crystallization of the VLDPE, a polymer that has a very broad crystallization range (see Fig. 1). For the ULDPE/iPP blends the behavior was qualitatively similar to the VLDPE/iPP blends.²²

The 80 : 20 blends without sorbitol in Figure 5 only exhibit their increase in G' at lower temperatures (at 109.1°C and 108.9°C for the LLDPE/iPP and the VLDPE/iPP blends respectively, see Table III) than iPP or the blends with sorbitol, as expected from its fractionated crystallization behavior. These blends crystallize at temperatures that are higher than that of pure PE (LLDPE and VLDPE) corroborating the nucleation effect of the iPP on the PE suggested by the DSC results that demonstrated the coincident crystallization of the dispersed phase and the matrix (see Table III and Fig. 4).

Figure 6 compares in the same plot, cooling curves obtained by RDA and DSC for LLDPE/iPP blends with and without sorbitol. The correspondence between the two techniques is excellent and the rheological effect of the fractionated crystallization is apparent when curves without sorbitol [Fig. 6(a)] and with sorbitol are compared [Fig. 6(b)]. In the case of the blend with sorbitol, the full crystallization of the 20% iPP in the PE matrix was followed by both techniques in view of the differences in crystallization temperatures between blend components induced by the nucleating agent.

If it is considered that the change in G' is directly proportional to crystallinity, the DSC data can be partially integrated as a function of temperature and compared to the RDA data as performed above in the case of the pure polymers (Fig. 2). Figure 7 shows such a plot; the difference with Fig. 2 is that the DSC data y-axis is expressed as percentage of material converted to solid, since being an immiscible blend, it would be difficult to calculate a percentage crystallinity. One could assume an additive mixing rule for the enthalpy of crystallization, but that would not reflect changes in the blends with sorbitol where at high temperatures only iPP can crystallize. In any

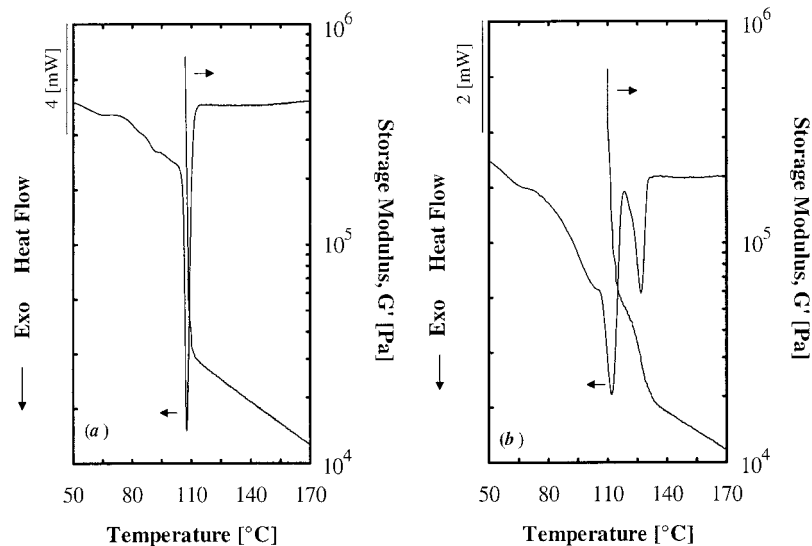


Figure 6 DSC curves and storage modulus G' (5 rad s^{-1} , 1% strain) versus temperature during cooling at $5^\circ\text{C}/\text{min}$ for LLDPE/iPP/sorbitol blends: (a) 80 : 20 : 0 and (b) 80 : 20 : 0.1.

case the correspondence between the DSC and the RDA data after a proper selection of the y -axis scale is very good up to the temperature at which the RDA run had to be stopped in view of the saturation of the normal force measurement. In Figure 7(a) the runs were stopped when the LLDPE matrix started to crystallize (for the blend with sorbitol) or when both components crystallized simultaneously (for the blend without sorbitol that exhibits coincident crystallization). In the case of the VLDPE/iPP blends, the results are qualitatively similar but we were able to follow the entire crystallization process not only of the dispersed iPP but also of the matrix, VLDPE, since this copolymer possesses an excess of rubbery chains at the testing temperatures (the degree of crystallinity of VLDPE is $\sim 20\%$ by weight at room temperature). So, in this case, the RDA was able to register the individual crystallization of the blend components in the sample with sorbitol or the start of the crystallization process of iPP and the subsequent coincident crystallization with VLDPE for the sample without sorbitol as described above [Fig. 4(b)].

Finally, the effectiveness of the nucleating agent sorbitol in stopping the fractionated crystallization of the iPP can also be demonstrated by dynamic rheological measurements, as shown in Figure 8. This figure presents complex viscosity measurements performed at temperatures at which both components are molten in the 80 : 20 LLDPE/iPP blend in view of the fractionated crystallization behavior of the iPP. When sorbitol is

added it induces the crystallization of the iPP at much higher temperatures [Fig. 2(a)] that are in the range of the rheological measurements. Figure 8 shows how at 120°C the complex viscosity is much greater for the sample with sorbitol than for the sample without nucleating agent, since the iPP has already crystallized at that temperature in the sample with sorbitol but is still molten in the blend without sorbitol. The differences in complex viscosity between the samples with and without sorbitol decrease as the temperature increases, and only disappear at 150°C when for both cases the samples are completely molten. It should be noted that while the measurements of Figure 8 at 150°C were all performed at conditions that guarantee linear viscoelastic behavior, those at lower temperatures (at least for samples with sorbitol) were not, because the crystallization of the dispersed phase is a transient phenomenon during cooling. Therefore, the curves of Figure 8 can only be compared qualitatively. This effect is currently being studied in our laboratory.

The results presented here could have practical implications for immiscible blends that exhibit the phenomenon of fractionated crystallization, since it is clear that they are solidifying at much lower temperatures than the samples that contain a suitable nucleating agent.

CONCLUSIONS

The results obtained in this work corroborated previous findings that indicated that under dy-

dynamic cooling conditions, the onset of crystallization could be followed by dynamic rheological measurements. In the range of frequencies and applied strains explored in this work we found no significant effect on the onset of crystallization of the resins employed (iPP, LLDPE, and ULDPE). The only limitations encountered were at very low frequencies and depended on the crystallization rate of the polymers employed.

On the other hand, the dynamic rheological measurements were found to be a useful tool to study the phenomenon of fractionated crystallization. In case the crystallization of iPP fine droplets in a PE matrix is to be followed completely, either a nucleating agent must be used (in order to increase the crystallization temperature of iPP eliminating the fractionated crystallization of the droplets), or a matrix with a low enough viscosity

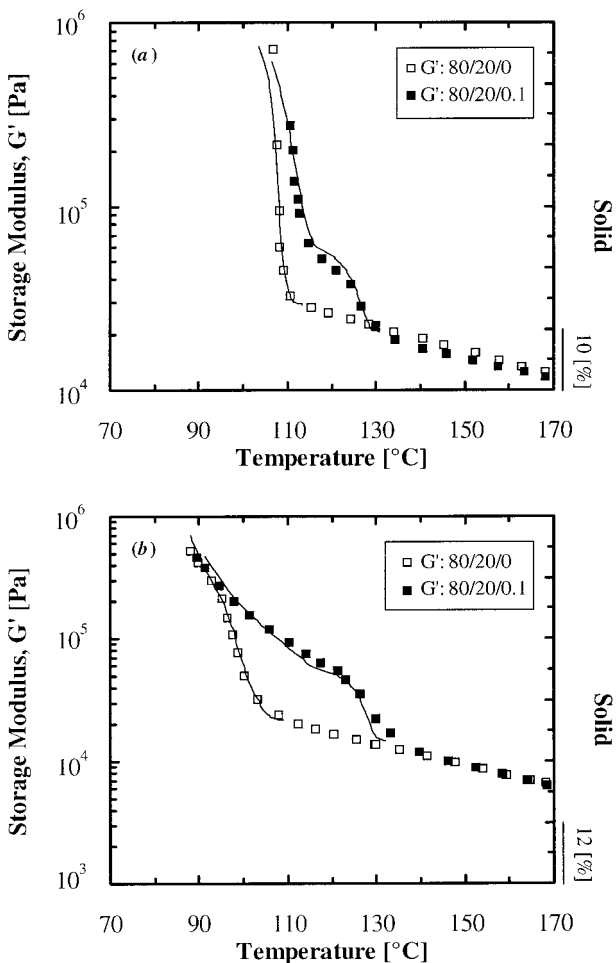


Figure 7 DSC-derived solid conversion curves (solid line) and storage modulus G' at 5 rad s^{-1} and 1% strain (symbols) versus temperature during cooling at $5^{\circ}\text{C}/\text{min}$ for blends: (a) LLDPE/iPP/sorbitol and (b) VLDPE/iPP/sorbitol.

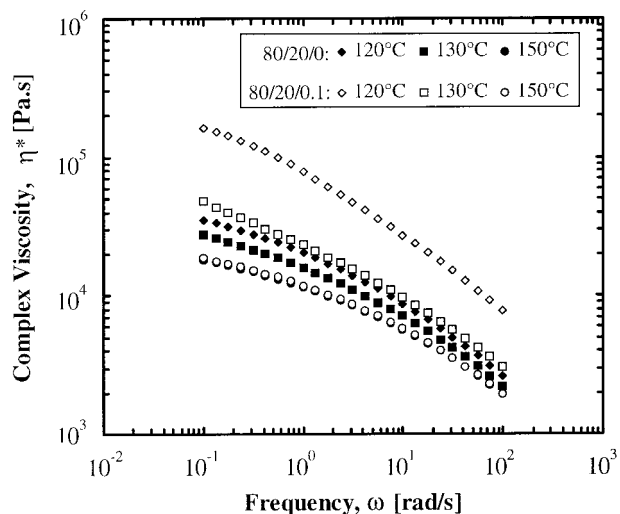


Figure 8 Complex viscosity η^* versus frequency of LLDPE/iPP/sorbitol blends at different temperatures at 15% strain.

in the temperature range where fractionated crystallization occurs must be used (like VLDPE or ULDPE). The crystallization behavior of iPP/branched PE blends studied by dynamic rheological techniques yielded results that were in close agreement with parallel DSC measurements; this was demonstrated by a direct comparison between calorimetrically measured solid conversion and G' changes as a function of temperature. At the same time, the results obtained here demonstrate the rheological consequences of the onset of crystallization in heterogeneous systems where fractionated crystallization was present.

The authors acknowledge the financial support of the Consejo Venezolano de Investigaciones Científicas y Tecnológicas (CONICIT) through Grant NM-43 (Proyecto Nuevas Tecnologías, BID-CONICIT). We also thank F. Ciardelli and C. Bruni from the University of Pisa (Italy) for providing the very and ultra low density polyethylene.

REFERENCES

1. Y. S. Lipatov, V. F. Shumasky, I. P. Getmanchuk, and A. N. Gorbatenko, *Rheol. Acta*, **21**, 270 (1982).
2. J. W. Teh, H. P. Blom, and A. Rudin, *Polymer*, **35**, 1680 (1994).
3. Y. G. Lin, D. T. Mallin, J. C. W. Chien, and H. H. Winter, *Macromolecules*, **24**, 850 (1991).
4. Y. P. Khana, *Macromolecules*, **26**, 3639 (1993).
5. C. Carrot, J. Guillet, and K. Boutahar, *Rheol. Acta*, **32**, 566 (1993).

6. R. Shroff, A. Prasad, and C. Lee, *J. Polym. Sci., Polym. Phys. Ed.*, **34**, 2317 (1996).
7. R. Hingmann, J. Rieger, and M. Kersting, *Macromolecules*, **28**, 3801 (1995).
8. L. Mandelkern, in *Physical Properties of Polymers*, ACS Professional Reference Book (American Chemical Society), Washington, DC, 1993, Chap. 4.
9. D. Vesely, in *Polymer Blends and Alloys*, M. J. Folkes and P. S. Hope, Eds., Chapman & Hall, Cambridge, 1993, Chap. 5.
10. U. W. Gedde, *Polymer Physics*, Chapman & Hall, London, 1995.
11. G. D. Wignall, in *Physical Properties of Polymers*, ACS Professional Reference Book (American Chemical Society), Washington, DC, 1993, Chap. 7.
12. J. M. Dealy and K. F. Wissbrum, *Melt Rheology and its Role in Plastics Processing, Theory and Applications*, Van Nostrand Reinhold, New York, 1989, Chap. 2.
13. H. Frensch, P. Harnischfeger, and B. J. Jungnickel, in *Multiphase Polymers: Blends and Ionomers*, L. A. Utracki, and R. A. Weiss, Eds., ACS Symposium Series 395, 1989, Chap. 5.
14. O. T. Ikkala, R. M. Holsti-Miettinen, and J. Sepälä, *J. Appl. Polym. Sci.*, **49**, 1165 (1993).
15. T. Tang and B. Huang, *J. Appl. Polym. Sci.*, **53**, 355 (1994).
16. O. O. Santana and A. J. Müller, *Polym. Bull.*, **32**, 471 (1994).
17. A. C. Manaure, J. J. Sánchez, J. Rotino, J. L. Rojas, C. Latorre, G. Mendez, and A. J. Müller, *Proceedings of the 2nd SIAP / 4th SLAP / 6th IMC*, Gramado, Brasil, 1994, p. 205.
18. R. A. Morales, M. L. Arnal, and A. J. Müller, *Polym. Bull.*, **35**, 379 (1995).
19. M. L. Arnal and A. J. Müller, *Proceedings of the 3rd Congresso Brasileiro de Polimeros*, Rio de Janeiro, Brasil, 1995, p. 530.
20. A. J. Müller, A. C. Manaure, J. J. Sánchez, G. Mendez, C. Bruni, and F. Ciardelli, *Proceedings of the 3rd Congresso Brasileiro de Polimeros*, Rio de Janeiro, Brasil, 1995, p. 639.
21. A. C. Manaure, R. A. Morales, J. J. Sánchez, and A. J. Müller, *Proceedings of the 3rd SIAP / 5th SLAP*, Mar de Plata, Argentina, 1996, p. 205.
22. A. C. Manaure, R. A. Morales, J. J. Sánchez, and A. J. Müller, *Proceedings of SPE, ANTEC '97*, Toronto, Canada, 1997, p. 3780.
23. M. L. Arnal, A. Covuccia, and A. J. Müller, *Proceedings of SPE, ANTEC '97*, Toronto, Canada, 1997, p. 3775.
24. A. Sánchez, C. Rosales, and A. J. Müller, *Proceedings of SPE, ANTEC '97*, Toronto, Canada, 1997, p. 3761.
25. M. E. Matos, C. Rosales, A. J. Müller, and B. D. Favis, *Proceedings of SPE, ANTEC '97*, Toronto, Canada, 1997, p. 2552.
26. A. C. Manaure and A. J. Müller, *J. Appl. Polym. Sci.* (to be submitted)
27. A. J. Müller and V. Balsamo, in *Advances in Polymer Blends and Alloys Technology*, Vol. 5, K. Finlayson, Ed., Technomic Publishing Co., Inc., 1994, Chap. 1.
28. B. Wunderlich, *Thermal Analysis*, Academic Press Inc., New York, 1990.
29. P. L. Joskowicz, A. Muñoz, J. Barrera, and A. J. Müller, *Macromol. Chem. Phys.*, **196**, 385 (1995).
30. V. B. F. Mathot and M. F. J. Pijpers, *J. Appl. Polym. Sci.*, **39**, 979 (1990).